Fatty acid – functionalized cellulose nanocomposites for vat photopolymerization

Fatty Acid – Functionalized Cellulose Nanocomposites for Vat Photopolymerization

Mirko Maturi[a], Chiara Spanu[a], Natalia Fernández-Delgado[b], Sergio I. Molina[b], Mauro Comes Franchini[a], Erica Locatelli[a], Alberto Sanz de León*[b]*

[a] *Department of Industrial Chemistry "Toso Montanari", University of Bologna, Viale Risorgimento 4, 40136 Bologna, Italy.*

[b] *Dpto. Ciencia de los Materiales, I. M. y Q. I., IMEYMAT, Facultad de Ciencias, Universidad de Cádiz, Campus Río San Pedro, s/n, 11510 Puerto Real (Cádiz), Spain.*

CORRESPONDING AUTHORS:

Erica Locatelli: erica.locatelli2@unibo.it

Alberto Sanz de León: alberto.sanzdeleon@uca.es

KEYWORDS: nanocellulose, surface modification, fatty acids, vat photopolymerization, additive manufacturing.

ABSTRACT

In recent years, nanocellulose, also called cellulose nanocrystals (CNCs), arose as one of the most interesting bio-based material for the incorporation as additive in polymers, due to its ability to increase the mechanical properties of the derived nanocomposites. Unfortunately, the natural hydrophilicity of CNCs strongly limited the mutual dispersion of cellulose crystals into the polymeric lipophilic chains, posing huge limitations both in cellulose loadings and efficacy. Herein we have synthesized a series of nanocomposites for vat photopolymerization, based on a commercial resin and cellulose nanocrystals (CNCs) modified with fatty acids obtained from safflower oil (SOFA), which allow hydrophobization of CNCs and their proper dispersion in the polymeric resin. The combination of these compounds allows manufacturing solid and complex objects without any defects in their structure from bio-based nanocomposites with CNCs-SOFA concentrations up to 5 wt.%. The analyses of their mechanical and optical properties were also studied revealing that nanocomposites with CNCs-SOFA possess increased stiffness and strength without experiencing a significant loss in their transparency, when compared to the pristine resin.

1. INTRODUCTION

Nanocellulose, obtained from mild acid-hydrolysis of cellulose, is the most abundant and renewable biopolymer on earth making it a promising material for various purposes. In particular, its high crystallinity has been explored and exploited for the enormous increment of mechanical properties of polymers when used as additive in composites materials. [1] However, the presence of a large amount of hydroxyl groups often leads to precipitation of cellulose nanocrystals (CNCs) in non-aqueous solvents, leading also to poor dispersion in most of the polymeric matrix. For this reason, various different surface functionalization approaches have been reported in the literature. [2,3] The hydrophobization of CNCs is extremely important in the production of nanocellulose-based composites. In order to hydrophobically modify the CNCs, the exploitation of the surface hydroxyl groups for introducing long hydrophobic chains has been seen to be the most effective approach. [4] To achieve this goal, the esterification reaction between CNCs hydroxyl groups and carboxylic acids, acid anhydrides or acyl chlorides has been used to introduce hydrophobic functional groups onto CNCs surface, often using pyridine as a basic solvent. [5] Commonly, dodecanoyl chloride or other long chain, commercially available, fatty acids chlorides have been employed as hydrophobic surface modifiers, due to their low cost and high availability. [6] Anyway, green alternatives, derived directly from the natural pool, have found scarce investigation as hydrophobic modifier, probably due to the presence of different molecules in the same mixture, thus making difficult to control both the reactions and the final products. For instance, vegetable oils, which are indeed mixture of long chain fatty acid esters of glycerol, may represent an excellent, cheap and bio-based source of hydrophobic ligands to be used as cellulose hydrophobizers. Stark and co-workers exploited the transesterification of canola oil fatty acid methyl esters in order to functionalize CNCs surface. [7] However, their approach required harsh conditions such as employing a large excess of fatty acids and applying high vacuum and high temperatures for prolonged times with a strict control on the degree of vacuum applied and on the stirring speed of the reaction, strongly hindering the possibility to scale up the reaction.

Indeed, safflower oil, composed of linoleic (82%), oleic (10%), palmitic (4%), stearic (2%), and linolenic acid (0.5%) is a promising candidate due to its peculiar composition, since it is almost entirely composed of a single fatty acid (linoleic acid), whereas other oils present more components and in more variable percentages. [8] Moreover, it is abundant and present all over the world, but it is commonly used only as minor components in cosmetics or as flavouring agent in food, and not in quantities able to saturate its market: therefore, it may represent a good candidate for modification of CNCs.

CNCs possess interesting structural properties, with reported stiffness and strength values of 10-100 GPa and 300-6000 MPa respectively [9,10], so they are widely used in the development of more sustainable composite materials, contributing to the circular economy. For decades, different authors have reported to obtain nanocomposites with enhanced mechanical [11], optical [12], or stimuli-responsive [13] properties with 0.1-10 wt.% CNC contents using biodegradable polymers as PLA [14], PVA [15], or PCL [16]. In the latest years, with the rise of the additive manufacturing techniques, more and more studies of nanocomposites prepared with this technology are also reported. [17–19] Noteworthy, since CNCs are highly hydrophilic, many authors report the necessity of performing a surface modification treatment prior to the manufacturing of the composites to increase the compatibility between the CNCs and the hydrophobic polymer matrix. [20–22] In many of these cases these modifications include fossil-fuel derived compounds, which makes the general manufacturing process less sustainable. [23] The incorporation of pristine CNCs into photocurable resins for vat photopolymerization, including stereolithography and digital light processing (DLP), has been already reported in the recent literature, but this approach showed strong limitations in the amount of loadable nanomaterial and it required harsh conditions for the incorporation of the nanofiller into the liquid monomer mixtures. [17,24,25]

Here we present an easy and scalable approach for the surface modification of CNCs with fatty acids isolated from safflower oil employing their acyl chlorides, and its application as an additive in resins for vat photopolymerization. The hydrophobization of the CNCs increased their compatibility with

the resin, generating a good dispersion of the nanocrystals within the polymeric matrix. Their use in the development of complex structures by additive manufacturing allowed synthesizing a series of cellulose-based nanocomposites, which presented enhanced mechanical properties and high transparency. This paves the way towards the development of new bio-based materials suitable for additive manufacturing technologies as a greener alternative to the current composite materials. [26–28]

2. MATERIALS AND METHODS

All chemicals were purchased from Sigma-Aldrich Co. (St Louis, MO, USA) and used as received. Sulfonated cellulose nanocrystals (CNCs) have been prepared by acid hydrolysis of Whatman® ashless cellulose filters as previously described by some of us, using H_2SO_4. [29] The photocurable resin used for vat photopolymerization (eResin-PLA) was purchased from eSun (Shenzhen, China).

2.1 Isolation of fatty acids from oil

In a 1 L round bottomed flask, 200 g of safflower oil were added to a solution prepared by dissolving 50 g of KOH in 50 mL in water, followed by the addition of 350 mL of ethanol. The mixture was refluxed for 15 minutes, after which it was cooled down to room temperature and acidified with a solution composed of 50 mL of sulfuric acid diluted with 200 mL of ice. The obtained safflower oil fatty acids (SOFA) were then extracted three times with 500 mL of hexane or petrol ether; next, the combined organic phases were dried over Na_2SO_4 and the solvent was evaporated to afford the liquid mixture of fatty acids.

2.2 Fatty acid chlorides (SOFACs) and functionalization of CNCs

In a flame-dried 500 mL round-bottomed flask under N_2 flow and vigorous magnetic stirring, 70 mL of thionyl chloride (965 mmol, 2.85 eq.) were added to 120 g of SOFA (approximated to be composed of linoleic acid only, 428 mmol, 1.25 eq.). The mixture was refluxed for 30 min, during which it

turned from yellow to dark brown/black. After cooling down the mixture, the excess of thionyl chloride was removed *in vacuo* to afford the safflower oil fatty acid chlorides (SOFACs) as a brown liquid.

In parallel, 55 g of freeze-dried sulfonated CNCs (340 mmol of glucose repeating units, 1.0 eq) were dispersed in 1.5 L of DMF (previously dried by standing for 24 h on activated 3Å molecular sieves) under inert atmosphere. The SOFACs were added dropwise to the CNCs suspension, and the esterification reaction was allowed to take place by stirring overnight at 80°C.

Then, the excess of acyl chloride was quenched by adding 500 mL of isopropanol. Fatty-acid functionalized CNCs (CNCs-SOFA) were recovered by centrifugation (15 min at 4000 rpm) and washed isopropanol until a clear supernatant is obtained. The purified product was collected with a small amount of dichloromethane, which was then evaporated under vacuum. CNCs-SOFA were then obtained as a thin brown powder.

2.3 Determination of the degree of functionalization via the iodine number

An excess of standard Wijs solution (0.1 N ICl in acetic acid, 25 mL) was added to an aliquot of the oil samples (0.13–0.15 g) or of CNCs or CNCs-SOFA powder (around 1 g), that were weighed precisely, dissolved in 20 mL of cyclohexane/acetic acid 1:1. The prepared solutions were left to incubate for 1 h in the dark; then, 20 mL of a potassium iodide solution (100 g/L) and 150 mL of distilled water were added. The developed iodine was titrated using a 0.1000 M $Na_2S_2O_3$ standard solution.

2.4 Additive manufacturing of the nanocomposites

Nanocomposite precursors were prepared by mechanical dispersion in the eResin-PLA photopolymer resin (RPLA). 0.125 - 2.500 g of either CNCs or CNCs-SOFA were added into a small amount of resin (ca. 10 mL) and then vortexed at 3000 rpm for at least 1 min. Then, the mixture was stirred at 1500 rpm for at least 30 min to ensure a homogeneous dispersion without formation of air bubbles. The mixture was diluted to a final volume of 50 mL, suitable for the 3D-printer vat, having

nanocomposite precursors with CNCs or CNCs-SOFA concentrations ranging from 0.25 to 5 wt.%. Computer-assisted design (CAD) files of 1BA tensile testing specimens according to ASTM D638 and complex structures such as hollow cubic lattices (10 x 10 x 10 mm^3) were loaded using the XYZware Nobel software and a GCODE file, suitable for 3D-printing, was created. The precursors were poured into the vat of the stereolithography 3D-printer (Nobel 1.0, XYZprinting Inc.) and the objects were manufactured using a 405 nm laser with an output power of 100 mW, an XY resolution of 300 µm and a layer height of 25 - 100 µm. Printed objects were then detached from the printer platform and washed with isopropyl alcohol for at least 15 min. Post-processing of the samples was performed for 60 min in a UV chamber equipped with a light source of 405 nm and power of 1.25 mW/cm^2 (FormCure, Formlabs), previously heated at 60 ºC.

2.5 Characterization

ATR-FTIR analysis were performed using a Cary 630 FTIR spectrometer (Agilent). SEM images were acquired with a field emission gun scanning transmission electron microscope ZEISS LEO Gemini 1530 (FEG-STEM) and a FEI Nova NanoSEM 450 microscope equipped with a field-emission gun. Samples were previously sputtered with a few nm layer of Au in a Balzers SCD 004 Sputter Coater. High angle annular dark field (HAADF) STEM images were acquired by FEI Talos F200X G2 microscope. The CNCs and CNCs-SOFA samples were deposited onto a holey carbon grid for the HAADF-STEM analysis. XRD analysis was performed on a Philips PW 1050/81 spectrometer with a PW 1710 chain counting. A nickel filter of 0.15418 mm was used to make monochromatic the Cu(Kα) radiation. The acquisition region was 5° < 2 theta < 80°, with steps of 0.1° and count of intensity every two seconds. The range of analysis was 20° < 2 theta < 80° with a scanning rate of 0.05 °/s and time-per-step = 1 s. Contact angle measurements of CNCs and CNCs-SOFA were done on films of the lyophilized powders dispersed on a double-sided tape using deionized water in an FDM-printed goniometer. A coupled digital microscope was used to capture the images of the water droplets and the results were analyzed using the contact angle plugin of the ImageJ software. Tensile testing of the printed specimens was performed in a universal testing

machine (Shimadzu) at a constant speed of 1 mm/min, according to ASTM D638. At least 5 specimens were tested for each material. Young's modulus, tensile strength and elongation at break values were dissected for each one of the measured specimens. Results were averaged and standard deviations were presented as error bars. Transparency of the materials was characterized by measuring the transmitted light through 2.0 mm thickness films of the pristine resin and the nanocomposites in a range of wavelengths λ from 300 to 800 nm using a Varian Cary 50 Conc UV-Vis spectrophotometer.

3. RESULTS AND DISCUSSION

Safflower oil fatty acids (SOFAs) were firstly extracted from their triglycerides with a well consolidated alkali-mediated saponification followed by acidification and extraction with alkanes. In order to conjugate the fatty acids to the CNCs surface via ester bond, SOFAs were chlorinated using thionyl chloride, which is able to transform the carboxylic acid group of fatty acids into the corresponding fatty acid chlorides. Then, the functionalization of CNCs was performed in hot DMF (80°C), with no requirement for the presence of an additional tertiary base (**Figure 1**), even though triethylamine is sometimes employed in DMF to speed up the reaction. The functionalization of CNCs with acyl chlorides is traditionally performed in pyridine or triethylamine, which act both as solvent for the reaction and as bases for the removal of the HCl formed during the coupling. [30,31] However, pyridine shows important drawbacks related to its acute toxicity and volatility, while DMF represents a valuable alternative for acylation of CNCs. [32] Moreover, the thermal decomposition of DMF to $NHMe_2$ and CO allows for the in situ generation of the base required for the acyl chloride coupling to CNCs. [33] With this approach, the reaction is easily scalable, allowing for the production of around 40 g of functionalized CNCs per liter of solvent employed.

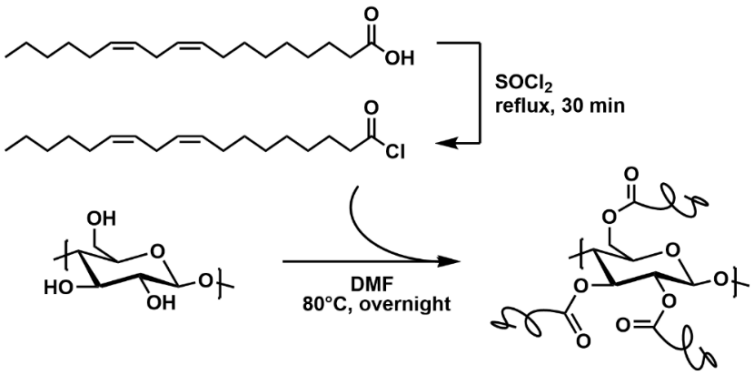

Figure 1. Schematic representation of the procedure for nanocellulose surface modification (only the major component of safflower oil, linoleic acid, is reported).

The morphology of CNCs was evaluated before and after their modification with fatty acids using SEM and HAADF-STEM (**Figure 2a-d)**). The SEM images revealed the presence of crystals with mean length of 1-2 μm before and after functionalization. The difference in the appearance of the whole sample in SEM images should be ascribed to the difference drying behaviour of functionalized versus pristine nanocellulose: indeed, functionalized CNCs tend to deposit better on the copper grid and to form a more uniform layer during the evaporation of the solvent, also thanks to a lower surface tension of organic solvents compared to water. The HAADF-STEM images showed that the individual nanocrystals possess similar morphology and size after the reaction with SOFAs, evidencing that the CNCs structure and size are maintained. In detail, lateral sizes of 250 nm - 6.5 μm and 650 nm - 6.6 μm were observed for CNCs and CNCs-SOFA, respectively.

In addition to the very different solvent dispersibility of CNCs-SOFA compared to pristine CNCs, the effectiveness of CNCs functionalization was assessed by ATR-FTIR spectroscopy (**Figure 2e)**), which revealed the appearance of distinctive absorption bands related to the fatty acid chains: a new peak at 1729 cm^{-1} can be attributed to the stretching of the carbonyl group in the ester moiety, and the peaks at 2895 cm^{-1} are related to the CH_2 in the fatty acid chain. Moreover, a reduction in the intensity of the O-H stretching band at 3320 cm^{-1} could be related to a lower concentration of hydroxyl groups, which have therefore reacted with the fatty acid chlorides.

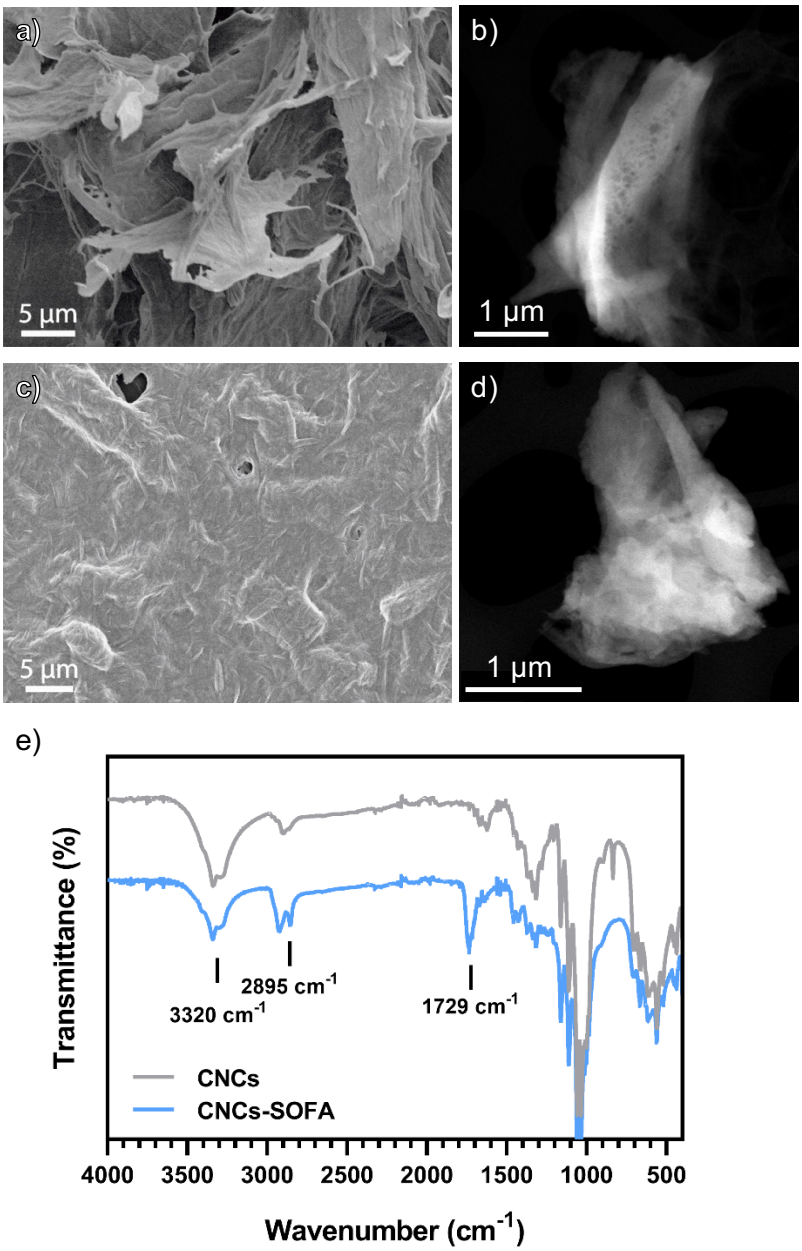

Figure 2. a) SEM and b) HAADF-STEM images of CNCs; c) SEM and d) HAADF images of CNCs-SOFA; e) comparison between the ATR-FTIR spectra of CNCs (grey) and CNCs-SOFA (blue).

Table 1. Functionalization parameters extracted using the Wijs method on CNCs-SOFA.

Iodine Value	22.3
mmol of double bonds / g of oil	0.897
g SOFA / g CNCs-SOFA	0.157
mmol SOFA / g CNCs	0.67
SOFA-functionalized OH groups	3.6 %

The degree of functionalization of the synthetized CNCs-SOFA was determined by evaluating the concentration of double bonds using the Wijs method for the determination of the iodine value. A comparison between the amount of iodine consumed by CNCs-SOFA and SOFAs alone gave the results summarized in **Table 1**. All the details of the quantitative assay are reported in the Supporting Information. Compared to the transesterification approach proposed by Stark,[7] who reported a degree of functionalization of 0.5 mmol fatty acid per gram of CNCs, this approach allowed for a 35% higher functionalization degree (0.67 mmol SOFA per gram of CNCs) using ten times less fatty acid derivatives, reducing significantly the waste of bio-based components. Therefore, even though the proposed approach exploits reagents and solvents (in particular $SOCl_2$ and DMF) that should be avoided in a green chemistry perspective, when compared to the synthetic pathways previously reported in the literature for acylation of CNCs, it represents one further step towards the development of greener alternatives for the extensive surface modification of CNCs.

Powder X-ray Diffraction (XRD) analysis was also performed on CNCs-SOFA to demonstrate the conservation of the crystallinity of CNCs after surface modification (**Figure S1**). The XRD spectra of the lipophilic material resembles all the features of pristine CNCs, suggesting that the functionalization with fatty acid chlorides was limited to the surface hydroxy groups. In addition, by comparing the peak at 22.6° in the two spectra, they are identical in terms of peak profile and full width at half maximum (FWHM). Since the peak width is directly related to the average crystallite size of the nanopowder, the XRD analysis suggests that the surface modification does not impact on the crystallite size, in agreement with SEM observations. The wettability of the CNCs and CNCs-SOFA was studied by contact angle. CNCs were highly hydrophilic, exhibiting water contact angles below 15 deg, and rapidly absorbing the water droplets in less than 1 s. After functionalization, the CNCs-SOFA became highly hydrophobic, with contact angles of 145 ± 4 deg.

Then, different amounts of CNCs or CNCs-SOFA were dispersed in the RPLA resin by high shear mixing and degassed under vacuum to achieve a homogeneous distribution of the crystals and avoid the presence of aggregates and air bubbles. The resin precursor was poured afterwards into the tank

and CAD files were loaded into the 3D-printer software. All the objects were successfully printed using concentrations up to 5.0 wt.% with either CNCs or CNCs-SOFA. The hollow cubic lattices and tensile testing specimens were successfully printed in all cases using layer heights of 100 µm, as shown in **Figure 3**. CNCs nanocomposites become moderately more translucent when the concentration increased, while CNCs-SOFA nanocomposites tend to turn slightly more yellow while keeping their transparency. The yellowing can be clearly observed for the 2 wt% CNCs-SOFA nanocomposites, while the other nanocomposites remain practically as colorless as the RPLA. The post-processing inside the UV chamber to ensure a full degree of cure of did not affect the transparency or color of any of the nanocomposites manufactured. These features will be discussed later on in detail when the optical properties of the nanocomposites are analyzed.

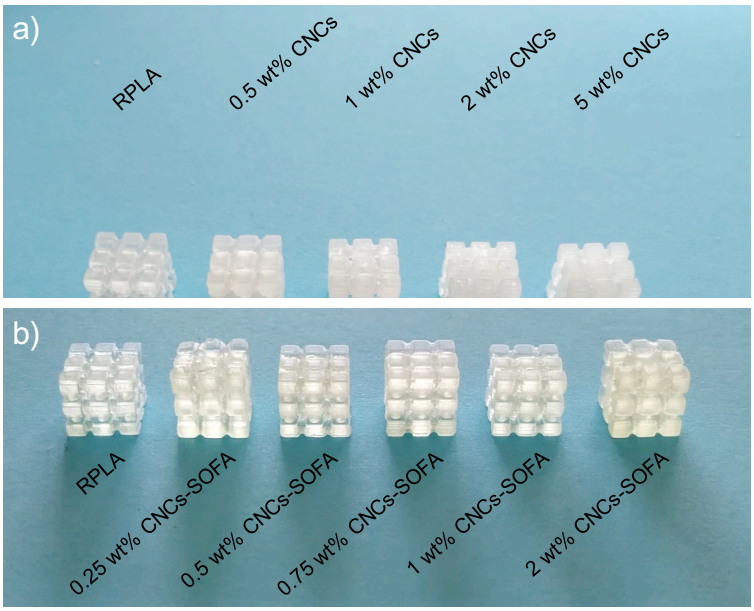

Figure 3. Digital photographs of 3D-printed cubic lattice objects with complex geometry using a) CNCs and b) CNCs-SOFA nanocomposites. The filler concentration increases from left to right. In both cases, the pristine resin (RPLA) is included as a reference. All the objects were printed using a layer height of 100 µm.

Moreover, **Figure S2** shows a small spacecraft printed with a 25 μm layer height and 2 wt.% CNCs nanocomposites, proving that high resolution can be achieved when printing complex objects. The range of concentrations that allowed the successful additive manufacturing of these materials is higher than what typically reported for other nanocomposites via vat photopolymerization, typically carbon-derived nanomaterials. These fillers, including graphite nanoplates, graphene oxide or carbon nanotubes highly absorb and scatter the laser light, hindering the proper polymerization of the composite [34–37]. In our study these scattering and absorbing events are minimized, since the CNCs are more transparent and present a refractive index of approximately 1.5, similar to that of the polymeric resins. Hence, this has allowed to print nanocomposites with CNCs contents up to 5 wt.%, compared to other vat photopolymerization composites where the maximum concentration achieved for complex structures is typically of 1 wt.% [34,38].

At least 5 tensile testing specimens of each nanocomposite were printed for mechanical characterization of the materials. Representative stress-strain curves are shown for CNCs and CNCs-SOFA nanocomposites in **Figure 4a,b)**. The characteristic mechanical parameters (Young's modulus, tensile strength and elongation at break) are dissected from these curves, averaged and presented in **Figure 4c-e)** for clearer interpretation of the tensile tests.

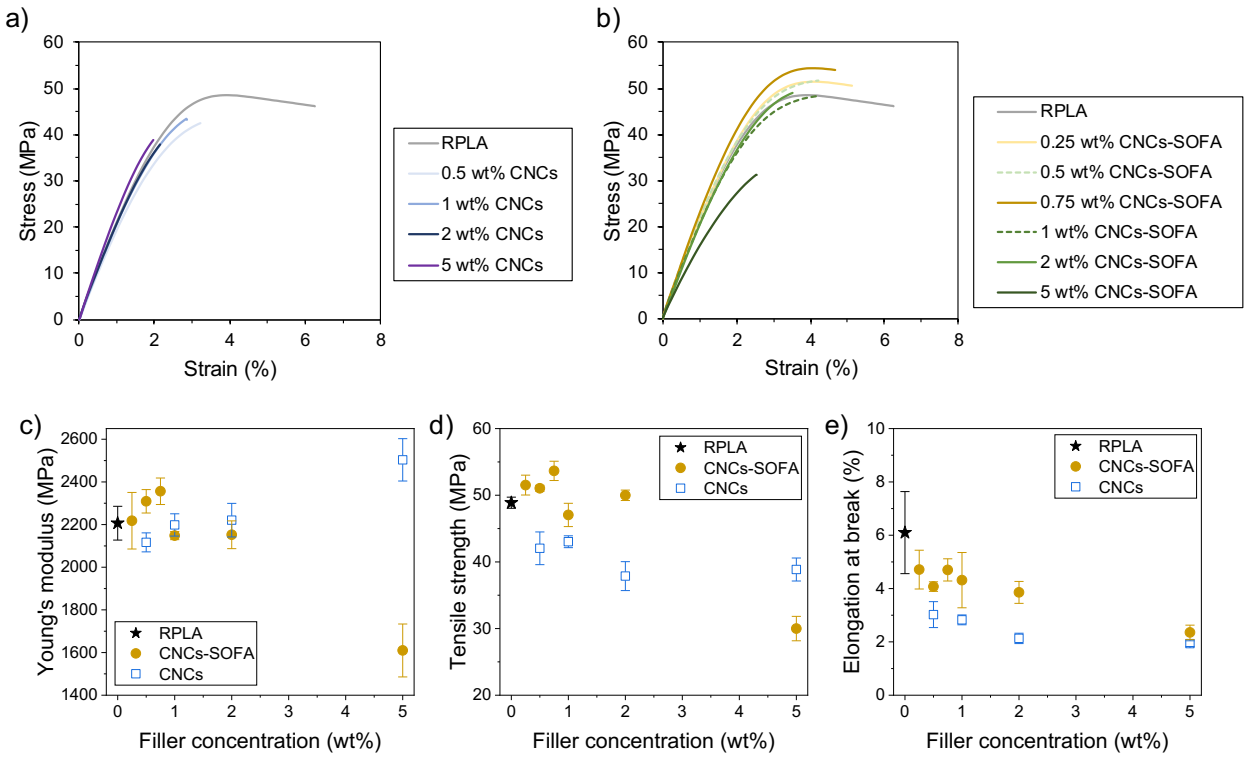

Figure 4. Representative tensile testing curves for a) CNCs and b) CNCs-SOFA nanocomposites. A tensile testing curve for pristine RPLA is presented in both graphs for direct comparison; average values of c) Young's modulus, d) tensile strength and e) elongation at break dissected from 5 independent measurements for pristine RPLA (black), CNCs nanocomposites (blue) and CNCs-SOFA nanocomposites (yellow).

These results show that nanocomposites prepared with unmodified CNCs are weaker than the pristine RPLA resin for the whole range of concentrations studied, due to the poor interaction between the hydrophobic resin and the hydrophilic CNCs. This is particularly clear for 5 wt.% CNCs nanocomposites, where the material becomes rigid (higher Young's modulus) but also much more fragile (lower elongation at break) due to the presence of a large number of CNCs that tend to agglomerate and act as nucleation points for material fracture. A similar effect has been previously observed by some of us in the manufacturing of graphite nanoplates nanocomposites for vat photopolymerization[36].

CNCs-SOFA nanocomposites on the other hand, exhibited enhanced stiffness and strength values, for CNCs-SOFA concentrations below 1 wt.%. The elongation at break, although also decreased with respect to the pristine RPLA resin, is always higher than that of CNCs nanocomposites with the same concentrations, indicating a much better compatibility with the resin, likely due to the hydrophobization of the CNCs with the fatty acids. The strong increase in hydrophobicity of CNCs when coated with SOFAs has shown to be able to increase the matrix-filler interactions by the formation of extensive intermolecular hydrophobic interaction, that allow for more efficient matrix-to-filler load transfer when the mechanical stress is applied to the 3D printed nanocomposite materials.

The density of the nanocomposites was also measured. In all cases, values between 1.08 and 1.25 g/cm^3 were obtained, with no differences observed between the nanocomposites and RPLA. This is most likely due to the fact that density of the resin (1.1 g/cm^3, according to the manufacturer) and the CNCs/CNCs-SOFA (1.5-1.6 g/cm^3) are quite similar, and the range of additive concentrations is rather low. Hence, the CNCs-SOFA also contributes to the development of lighter materials for structural applications, compared to other composites reinforced with inorganic fillers, which have a higher density.

These results are supported by the analysis of the fracture surface by SEM, as illustrated in **Figure 5**. They show that CNCs and CNCs-SOFA participate in the fracture mechanism, as different crystals can be appreciated in both fracture surfaces. The unmodified CNCs act as potential sites for the generation of cracks that lead to fracture surface, as pointed by the blue arrows in **Figure 5d)**, showing a gap between the CNCs and the resin, which evidences the poor compatibility between them. On the other hand, the fracture surface of the 0.5 wt.% CNCs-SOFA nanocomposites shows well-integrated CNCs-SOFA within the polymeric matrix (see orange arrows in **Figure 5f)**).

This behaviour is observed for all the concentrations studied in this work (**Figures S3-S4**), which indicates that they can participate in the fracture mechanism together with the resin, bearing higher loads, in agreement with the tensile testing results previously discussed. This effect was also reported

by Feng et al. [39] in CNCs composites manufactured by vat photopolymerization. In their case, they used lignin-coated CNCs, which enhanced their compatibility with the polymeric resin, increasing their mechanical properties for CNCs contents below 1 wt.%. Moreover, a similar aspect in the fracture surface was previously observed by some of us in cork-based nanocomposites, after functionalization with poly (butyl acrylate), supporting that hydrophobization of bio-based additives enhances the mechanical performance of the composites [40]. Other authors also reported on the successful additive manufacturing of CNCs nanocomposites via vat photopolymerization. For instance, Palaganas et al. [24] increased the mechanical properties of a poly(ethylene glycol) diacrylate (PEGDA) based resin when they were loaded with 0.3 wt.% CNCs. Wang et al. [41] reported on the grafting of the CNCs with maleic acid. They observed an increase in the tensile strength and modulus when the CNCs were added up to 2 wt.%. However, in these cases the maximum strengths and stiffness reported are below 20 MPa and 500 MPa, respectively, below the results reported in this work.

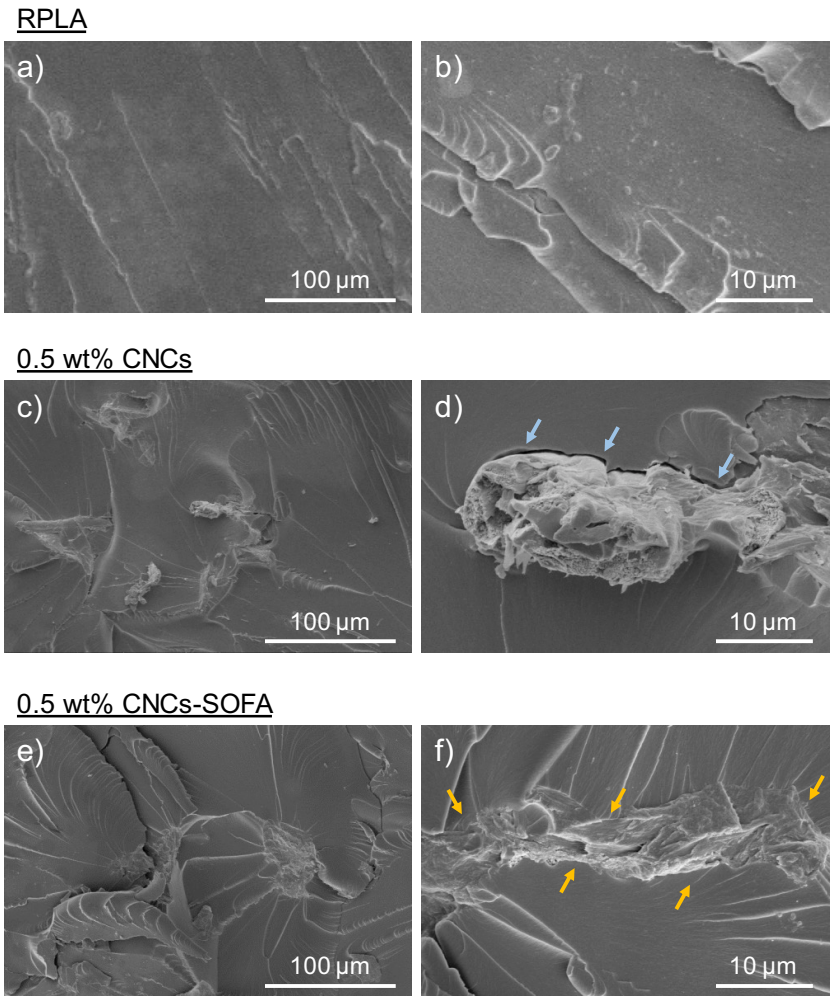

Figure 5. Fracture surface of the tensile testing specimens of a-b) pristine RPLA; c-d) 0.5 wt.% CNCs nanocomposites and e-f) 0.5 wt.% CNCs-SOFA nanocomposites. Blue arrows in d) show the presence of a fracture around a CNC due to its poor compatibility with the RPLA matrix, while orange arrows in f) evidence that CNCs-SOFA are well-integrated within the resin.

Finally, the transparency of these nanocomposites was measured. One of the advantages of using CNCs instead of carbon or ceramic based fillers is their transparency to visible light. This allows creating nanocomposites enhancing the mechanical properties of the polymer resins while keeping (i.e. not significantly reducing) their characteristic transparency. Many authors have reported this in the development of thin films, prepared by solvent casting or other conventional manufacturing technologies [42–44], but this is to the best of our knowledge the first work where all the advantages

of CNCs incorporation are kept and studied in objects 3D-printed by vat photopolymerization. In **Figure 6a-b)**, the transparency of the nanocomposites is presented as the transmitted light when a beam of visible light passes through 2 mm of material. It can be observed that the CNCs-SOFA nanocomposites are clearly more transparent than the CNCs nanocomposites. For instance, 5 wt.% CNCs-SOFA nanocomposites have transmittance values similar to those of 0.5 – 1 wt.% CNCs nanocomposites. This is likely caused by a better dispersion of the CNCs-SOFA in the RPLA matrix, favoured by the higher compatibility between the two compounds. This does not happen for CNCs nanocomposites, where the CNCs have a higher tendency to be dispersed in larger aggregates with sizes above the visible light wavelengths (400-700 nm), favouring the light scattering inside of the material due to internal reflection and diffraction events. This also expected to happen for CNCs-SOFA nanocomposites since the transmittance values also decrease when compared to the pristine RPLA, although to a much lesser extent. Indeed, no significantly differences in terms of transparency can be observed by the naked eye between RPLA and 0.5-1 wt.% CNCs-SOFA, as evidenced in **Figure 6c)**.

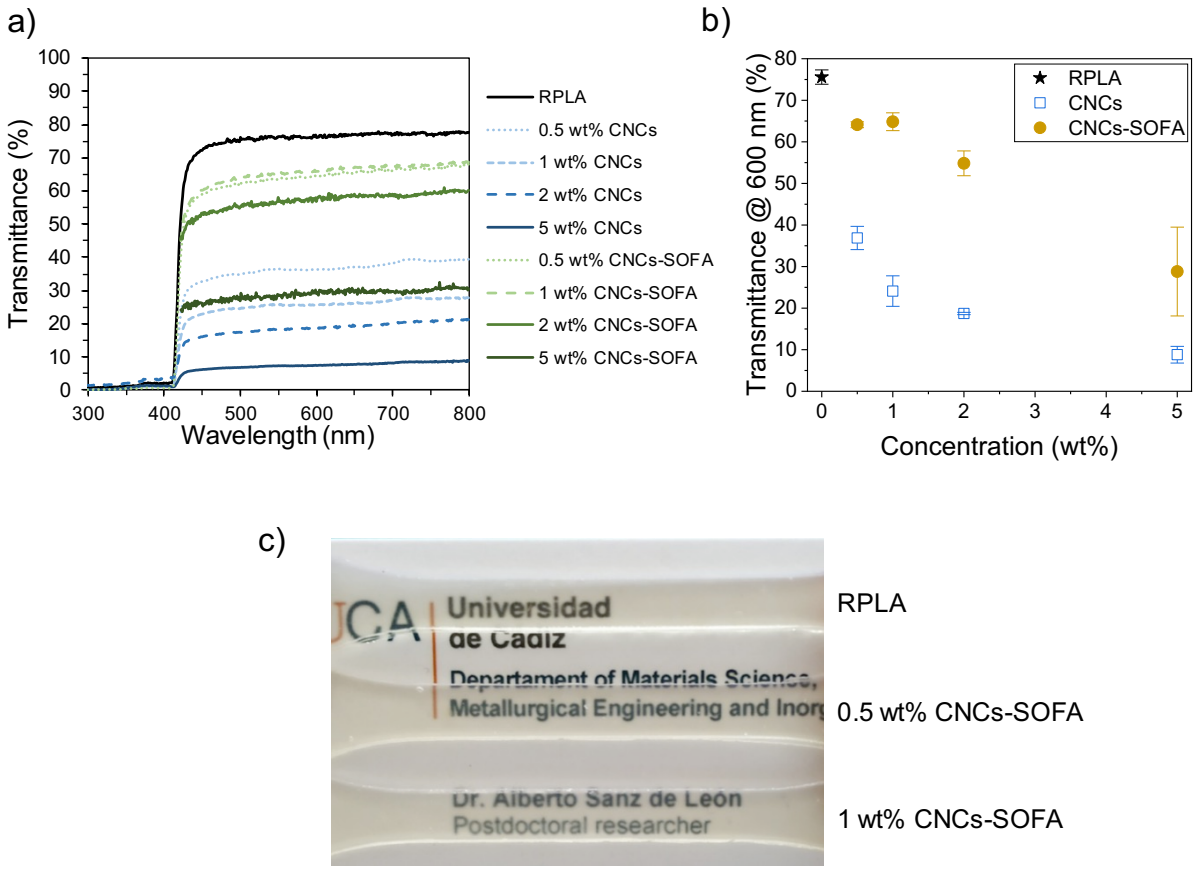

Figure 6. Transmittance values a) in the UV-Vis range and b) at λ = 600 nm of RPLA, CNCs and CNCs-SOFA nanocomposite films with 2 mm thickness; c) digital photographs of RPLA, 0.5 wt.% and 1 wt.% CNCs-SOFA nanocomposite films with 2 mm thickness evidencing their transparency under white light.

4. CONCLUSIONS

In this work we have developed a series of nanocomposites using a commercial resin and safflower fatty acid-modified CNCs. We have demonstrated that hydrophobized CNCs present a number of advantages compared to additives used in the past for additive manufacturing such as pristine CNCs and carbon based materials. Indeed, the CNCs are highly transparent so they can be used without affecting the polymerization of the resin due to absorption phenomena, as in case of carbon fibres,

nanoplatelets or nanotubes. Moreover, the good compatibility between the filler and the matrix, achieved by the hydrophobization of the CNCs by surface modification with SOFA, led to a good dispersion of the CNCs-SOFA in the RPLA matrix up to 5 wt.%. This in turn led to transparent nanocomposites with enhanced mechanical properties. These results, coupled with the bio-based nature of both CNCs and SOFA modifier represent a step forward towards the environmental sustainability of materials for vat photopolymerization and resins-additives.

AUTHORS CONTRIBUTIONS

Conceptualization MM, EL, ASdL; Data curation CS; Formal analysis CS; Funding acquisition SIM, MCF; Investigation MM, CS, NFD, ASdL; Methodology MM, EL, NFD, ASdL; Project administration SIM, MCF; Resources SIM, MCF; Software MM; Supervision SIM, ASdL, EL; Writing - original draft MM, CS, ASdL; Writing - review & editing EL, MCF.

ACKNOWLEDGEMENTS

This work was funded by Junta de Andalucía (Research group INNANOMAT, ref. TEP-946). The University of Bologna is also gratefully acknowledged. Co-funding from UE is also acknowledged. ASdL acknowledges the Ministry of Science, Innovation and Universities for his Juan de la Cierva Incorporación postdoctoral fellowship (IJC2019-041128-I). NFD also acknowledges co-founding by European Social Fund and Ministry of Economic Transformation, Industry, Knowledge and Universities of the Junta de Andalucía. SEM and STEM measurements were carried out at the DME-SC-ICyT-ELECMI-UCA.

REFERENCES

[1] A. Dufresne, Nanocellulose: a new ageless bionanomaterial, Mater. Today. 16 (2013) 220–227. doi:10.1016/j.mattod.2013.06.004.

[2] S. Tortorella, V. Vetri Buratti, M. Maturi, L. Sambri, M. Comes Franchini, E. Locatelli, Surface-Modified Nanocellulose for Application in Biomedical Engineering and Nanomedicine: A Review, Int. J. Nanomedicine. Volume 15 (2020) 9909–9937. doi:10.2147/IJN.S266103.

[3] Y. Habibi, Key advances in the chemical modification of nanocelluloses, Chem. Soc. Rev. 43 (2014) 1519–1542. doi:10.1039/C3CS60204D.

[4] S. Mondal, Review on Nanocellulose Polymer Nanocomposites, Polym. Plast. Technol. Eng. 57 (2018) 1377–1391. doi:10.1080/03602559.2017.1381253.

[5] J.D. Rusmirović, J.Z. Ivanović, V.B. Pavlović, V.M. Rakić, M.P. Rančić, V. Djokić, A.D. Marinković, Novel modified nanocellulose applicable as reinforcement in high-performance nanocomposites, Carbohydr. Polym. 164 (2017) 64–74. doi:10.1016/j.carbpol.2017.01.086.

[6] B.M. Trinh, T. Mekonnen, Hydrophobic esterification of cellulose nanocrystals for epoxy reinforcement, Polymer (Guildf). 155 (2018) 64–74. doi:10.1016/j.polymer.2018.08.076.

[7] L. Wei, U.P. Agarwal, K.C. Hirth, L.M. Matuana, R.C. Sabo, N.M. Stark, Chemical modification of nanocellulose with canola oil fatty acid methyl ester, Carbohydr. Polym. 169 (2017) 108–116. doi:10.1016/j.carbpol.2017.04.008.

[8] B. Bozan, F. Temelli, Chemical composition and oxidative stability of flax, safflower and poppy seed and seed oils, Bioresour. Technol. 99 (2008) 6354–6359. doi:10.1016/j.biortech.2007.12.009.

[9] S. Ling, W. Chen, Y. Fan, K. Zheng, K. Jin, H. Yu, M.J. Buehler, D.L. Kaplan, Progress in Polymer Science Biopolymer nanofibrils : Structure , modeling , preparation , and applications, 85 (2018) 1–56.

[10] Ansys Granta EduPack software, ANSYS, Inc., Cambridge, UK, 2021., (n.d.).

[11] V. Favier, H. Chanzy, J.Y. Cavaille, Polymer Nanocomposites Reinforced by Cellulose Whiskers, Macromolecules. 28 (1995) 6365–6367. doi:10.1021/ma00122a053.

[12] L. Tian, J. Luan, K.-K. Liu, Q. Jiang, S. Tadepalli, M.K. Gupta, R.R. Naik, S. Singamaneni, Plasmonic Biofoam: A Versatile Optically Active Material, Nano Lett. 16 (2016) 609–616. doi:10.1021/acs.nanolett.5b04320.

[13] C.J. R., S. Kadhiravan, T.D. J., R.S. J., W. Christoph, Stimuli-Responsive Polymer Nanocomposites Inspired by the Sea Cucumber Dermis, Science (80-.). 319 (2008) 1370–1374. doi:10.1126/science.1153307.

[14] S. Gazzotti, R. Rampazzo, M. Hakkarainen, D. Bussini, M.A. Ortenzi, H. Farina, G. Lesma, A. Silvani, Cellulose nanofibrils as reinforcing agents for PLA-based nanocomposites: An in situ approach, Compos. Sci. Technol. 171 (2019) 94–102. doi:https://doi.org/10.1016/j.compscitech.2018.12.015.

[15] S. Xu, M. Jiang, Q. Lu, S. Gao, J. Feng, X. Wang, X. He, K. Chen, Y. Li, P. Ouyang, Properties of Polyvinyl Alcohol Films Composited With Hemicellulose and Nanocellulose Extracted From Artemisia selengensis Straw , Front. Bioeng. Biotechnol. . 8 (2020).

https://www.frontiersin.org/article/10.3389/fbioe.2020.00980.

[16] Z. Moazzami Goudarzi, T. Behzad, L. Ghasemi-Mobarakeh, M. Kharaziha, An investigation into influence of acetylated cellulose nanofibers on properties of PCL/Gelatin electrospun nanofibrous scaffold for soft tissue engineering, Polymer (Guildf). 213 (2021) 123313. doi:https://doi.org/10.1016/j.polymer.2020.123313.

[17] S. Kumar, M. Hofmann, B. Steinmann, E.J. Foster, C. Weder, Reinforcement of stereolithographic resins for rapid prototyping with cellulose nanocrystals, ACS Appl. Mater. Interfaces. 4 (2012) 5399–5407. doi:10.1021/am301321v.

[18] S. Dinesh Kumar, K. Venkadeshwaran, M.K. Aravindan, Fused deposition modelling of PLA reinforced with cellulose nano-crystals, Mater. Today Proc. 33 (2020) 868–875. doi:https://doi.org/10.1016/j.matpr.2020.06.404.

[19] A. Rao, T. Divoux, C.E. Owens, A.J. Hart, Printable, castable, nanocrystalline cellulose-epoxy composites exhibiting hierarchical nacre-like toughening, Cellulose. 29 (2022) 2387–2398. doi:10.1007/s10570-021-04384-7.

[20] H.-M. Ng, L.T. Sin, T.-T. Tee, S.-T. Bee, D. Hui, C.-Y. Low, A.R. Rahmat, Extraction of cellulose nanocrystals from plant sources for application as reinforcing agent in polymers, Compos. Part B Eng. 75 (2015) 176–200. doi:https://doi.org/10.1016/j.compositesb.2015.01.008.

[21] B. Thomas, M.C. Raj, A.K. B, R.M. H, J. Joy, A. Moores, G.L. Drisko, C. Sanchez, Nanocellulose, a Versatile Green Platform: From Biosources to Materials and Their Applications, Chem. Rev. 118 (2018) 11575–11625. doi:10.1021/acs.chemrev.7b00627.

[22] D. Jia, J. Xie, M. Dirican, D. Fang, C. Yan, Y. Liu, C. Li, M. Cui, H. Liu, G. Chen, X. Zhang, J. Tao, Highly smooth, robust, degradable and cost-effective modified lignin-nanocellulose green composite substrates for flexible and green electronics, Compos. Part B Eng. 236 (2022) 109803. doi:https://doi.org/10.1016/j.compositesb.2022.109803.

[23] Y. Ren, J. Ma, W. Liu, C. Huang, C. Lai, Z. Ling, Q. Yong, Facile adjustment on cellulose nanocrystals composite films with glycerol and benzyl acrylate copolymer for enhanced UV shielding property, Int. J. Biol. Macromol. 204 (2022) 41–49. doi:https://doi.org/10.1016/j.ijbiomac.2022.01.168.

[24] N.B. Palaganas, J.D. Mangadlao, A.C.C. De Leon, J.O. Palaganas, K.D. Pangilinan, Y.J. Lee, R.C. Advincula, 3D printing of photocurable cellulose nanocrystal composite for fabrication of complex architectures via stereolithography, ACS Appl. Mater. Interfaces. 9 (2017) 34314–34324. doi:10.1021/acsami.7b09223.

[25] B. Wang, G. Ding, K. Chen, S. Jia, J. Wei, Y. Wang, R. He, Z. Shao, A physical and chemical double enhancement strategy for 3D printing of cellulose reinforced nanocomposite, J. Appl. Polym. Sci. 137 (2020) 1–11. doi:10.1002/app.49164.

[26] P. Sengsri, S. Kaewunruen, Additive manufacturing meta-functional composites for engineered bridge bearings: A review, Constr. Build. Mater. 262 (2020) 120535. doi:https://doi.org/10.1016/j.conbuildmat.2020.120535.

[27] A. Al Rashid, S.A. Khan, S. G. Al-Ghamdi, M. Koç, Additive manufacturing of polymer nanocomposites: Needs and challenges in materials, processes, and applications, J. Mater. Res. Technol. 14 (2021) 910–941. doi:https://doi.org/10.1016/j.jmrt.2021.07.016.

[28] X. Zhang, K. Zhang, L. Zhang, W. Wang, Y. Li, R. He, Additive manufacturing of cellular ceramic structures: From structure to structure–function integration, Mater. Des. 215 (2022)

110470. doi:https://doi.org/10.1016/j.matdes.2022.110470.

[29] S. Tortorella, M. Maturi, F. Dapporto, C. Spanu, L. Sambri, M. Comes Franchini, M. Chiariello, E. Locatelli, Surface modification of nanocellulose through carbamate link for a selective release of chemotherapeutics, Cellulose. 27 (2020) 8503–8511. doi:10.1007/s10570-020-03390-5.

[30] A. Bendahou, A. Hajlane, A. Dufresne, S. Boufi, H. Kaddami, Esterification and amidation for grafting long aliphatic chains on to cellulose nanocrystals: a comparative study, Res. Chem. Intermed. 41 (2015) 4293–4310. doi:10.1007/s11164-014-1530-z.

[31] J.R.G. Navarro, G. Conzatti, Y. Yu, A.B. Fall, R. Mathew, M. Edén, L. Bergström, Multicolor Fluorescent Labeling of Cellulose Nanofibrils by Click Chemistry, Biomacromolecules. 16 (2015) 1293–1300. doi:10.1021/acs.biomac.5b00083.

[32] T. Kuhnt, A. Herrmann, D. Benczédi, E.J. Foster, C. Weder, Functionalized cellulose nanocrystals as nanocarriers for sustained fragrance release, Polym. Chem. 6 (2015) 6553–6562. doi:10.1039/C5PY00944H.

[33] M.M. Heravi, M. Ghavidel, L. Mohammadkhani, Beyond a solvent: triple roles of dimethylformamide in organic chemistry, RSC Adv. 8 (2018) 27832–27862. doi:10.1039/C8RA04985H.

[34] Y. Li, Z. Feng, L. Huang, K. Essa, E. Bilotti, H. Zhang, T. Peijs, L. Hao, Additive manufacturing high performance graphene-based composites: A review, Compos. Part A Appl. Sci. Manuf. 124 (2019) 105483. doi:https://doi.org/10.1016/j.compositesa.2019.105483.

[35] K. Markandan, C.Q. Lai, Enhanced mechanical properties of 3D printed graphene-polymer composite lattices at very low graphene concentrations, Compos. Part A Appl. Sci. Manuf. 129 (2020) 105726. doi:https://doi.org/10.1016/j.compositesa.2019.105726.

[36] A.S. De León, S.I. Molina, Influence of the Degree of Cure in the Bulk Properties of Graphite Nanoplatelets Nanocomposites Printed via Stereolithography, Polymers (Basel). 12 (2020) 1103. doi:10.3390/polym12051103.

[37] C.Q. Lai, K. Markandan, B. Luo, Y.C. Lam, W.C. Chung, A. Chidambaram, Viscoelastic and high strain rate response of anisotropic graphene-polymer nanocomposites fabricated with stereolithographic 3D printing, Addit. Manuf. 37 (2021) 101721. doi:https://doi.org/10.1016/j.addma.2020.101721.

[38] A.S. de León, M. de la Mata, F.J. Delgado, S.I. Molina, Printable Graphene Oxide Nanocomposites as Versatile Platforms for Immobilization of Functional Biomolecules, Macromol. Mater. Eng. 307 (2022) 2100784. doi:https://doi.org/10.1002/mame.202100784.

[39] X. Feng, Z. Yang, S. Chmely, Q. Wang, S. Wang, Y. Xie, Lignin-coated cellulose nanocrystal filled methacrylate composites prepared via 3D stereolithography printing: Mechanical reinforcement and thermal stabilization, Carbohydr. Polym. 169 (2017) 272–281. doi:https://doi.org/10.1016/j.carbpol.2017.04.001.

[40] A.S. de León, F. Núñez-Gálvez, D. Moreno-Sánchez, N. Fernández-Delgado, S.I. Molina, Polymer Composites with Cork Particles Functionalized by Surface Polymerization for Fused Deposition Modeling, ACS Appl. Polym. Mater. 4 (2022) 1225–1233. doi:10.1021/acsapm.1c01632.

[41] B. Wang, J. Liu, K. Chen, Y. Wang, Z. Shao, Three-Dimensional Printing of Methacrylic Grafted Cellulose Nanocrystal-Reinforced Nanocomposites With Improved Properties,

Polym. Eng. Sci. 60 (2020) 782–792. doi:https://doi.org/10.1002/pen.25336.

[42] X. Xu, F. Liu, L. Jiang, J.Y. Zhu, D. Haagenson, D.P. Wiesenborn, Cellulose Nanocrystals vs. Cellulose Nanofibrils: A Comparative Study on Their Microstructures and Effects as Polymer Reinforcing Agents, ACS Appl. Mater. Interfaces. 5 (2013) 2999–3009. doi:10.1021/am302624t.

[43] N. El Miri, K. Abdelouahdi, A. Barakat, M. Zahouily, A. Fihri, A. Solhy, M. El Achaby, Bio-nanocomposite films reinforced with cellulose nanocrystals: Rheology of film-forming solutions, transparency, water vapor barrier and tensile properties of films, Carbohydr. Polym. 129 (2015) 156–167. doi:https://doi.org/10.1016/j.carbpol.2015.04.051.

[44] M. Yadav, F.-C. Chiu, Cellulose nanocrystals reinforced κ-carrageenan based UV resistant transparent bionanocomposite films for sustainable packaging applications, Carbohydr. Polym. 211 (2019) 181–194. doi:https://doi.org/10.1016/j.carbpol.2019.01.114.